analytical chemistry

TECHNICAL NOTE

pubs.acs.org/ac

Quantum Dots with Phenylboronic Acid Tags for Specific Labeling of Sialic Acids on Living Cells

Aiping Liu,[†,‡] Shuo Peng,[†] Jian Chow Soo,[†] Min Kuang,[§] Peng Chen,[†] and Hongwei Duan*[,†]

[†]School of Chemical and Biomedical Engineering, Nanyang Technological University, 70 Nanyang Drive, Singapore 637457

[‡]Department of Physics, Center for Optoelectronics Materials and Devices, Zhejiang Sci-Tech University, Xiasha College Park, Hangzhou 310018, China

[§]Ocean Nanotech, 2143 Worth Lane, Springdale, Arkansas 72764, United States

Supporting Information

ABSTRACT: Sialic acids with a nine-carbon backbone are commonly found at the terminal position of the glycans structures on cell membranes. The unique distribution and ubiquitous existence of sialic acid on the cell membrane make them important mediators in various biological and pathological processes. We report a new class of imaging probes based on semiconductor quantum dots with small molecular phenylboronic acid tags for highly specific and efficient labeling of sialic acid on living cells. Our results have shown that the use of these probes enables one-step labeling and continuous tracking of the cell surface sialic acid moieties without any pretreatment of living cells. The one-step procedure with fast binding kinetics and the biocompatibility of these probes make it an ideal noninvasive technology for living cell imaging. We also find that the labeled sialic acids undergo quick internalization shortly after surface binding via endocytosis and eventually distribute in the perinuclear region. This distribution pattern is consistent with the notion that sialylated glycoproteins are populated on cell membranes and recycled through the vesicular exocytotic and endocytic pathways. The superior photostability and brightness of quantum dots enable quantitative analysis of the diffusion dynamics of sialic acids, which has been a significant challenge for glycan imaging.

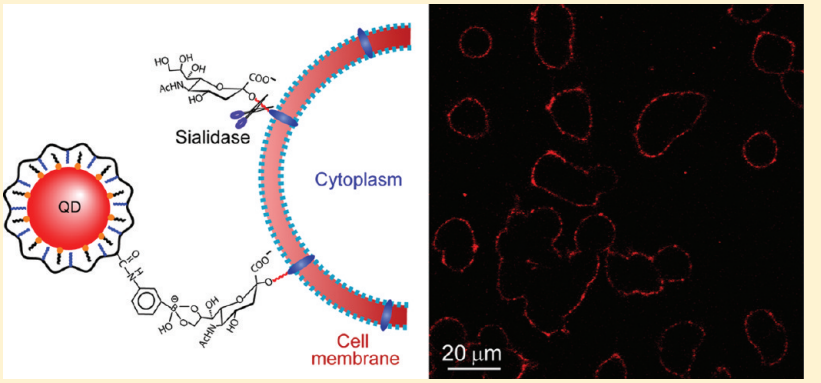

The complex array of glycans on the surface of mammalian cells plays essential roles in a variety of cell activities, for example, differentiation, proliferation, immune response, cell−cell communication, and microbial infection.[1] Among the diverse structures of glycans, sialic acids (SA) with a nine-carbon backbone are commonly found at the terminal position of the sugar chains. The unique distribution and ubiquitous existence of SA on the cell membrane make them important mediators in various biological and pathological processes.[2,3] Increasing evidence has revealed that changes in SA expression are closely associated with various disease states such as cancer, cardiovascular, and neurological diseases.[4−8] With the aim toward improved understanding on the complex glycosylation machinery and the development of glycotherapeutics for major human diseases, great efforts have been made to develop effective and low-toxic approaches for labeling SA on cell surfaces. Methods currently available are all involved with either in situ chemical modification of SA or incorporation of glycan analogues with bioorthogonal groups, i.e., azide through metabolic labeling, followed by chemical ligation and biological recognition to introduce fluorescent probes.[9−13] These multistep approaches are typically time-consuming, and the chemistries undertaken often suffer from high cytotoxicity and are not applicable for living cells.

Here, we report a new class of imaging probes based on semiconductor quantum dots (QD) with small molecular phenylboronic acid (PBA) tags, which allow highly specific and efficient labeling of SA on living cells. QDs exhibit unique optical properties such as size-tunable emission wavelength, broad excitation profiles, and superior photostability, which are not available from conventional fluorescent dyes and proteins.[14,15] Recent advances in QD synthesis and their surface chemistry have led to stable QD probes for molecular, cellular, and in vivo imaging.[16,17] For live cell imaging, the brightly stable fluorescence of QDs provides new possibilities for long-term tracking of protein diffusion and internalization at the single molecule level with high sensitivity. Although it remains a challenge to develop QDs for imaging targets inside living cells due to the lack of reliable methods to release trapped QDs from vesicles, significant success has been

Received: July 11, 2010
Accepted: December 9, 2010
Published: December 23, 2010

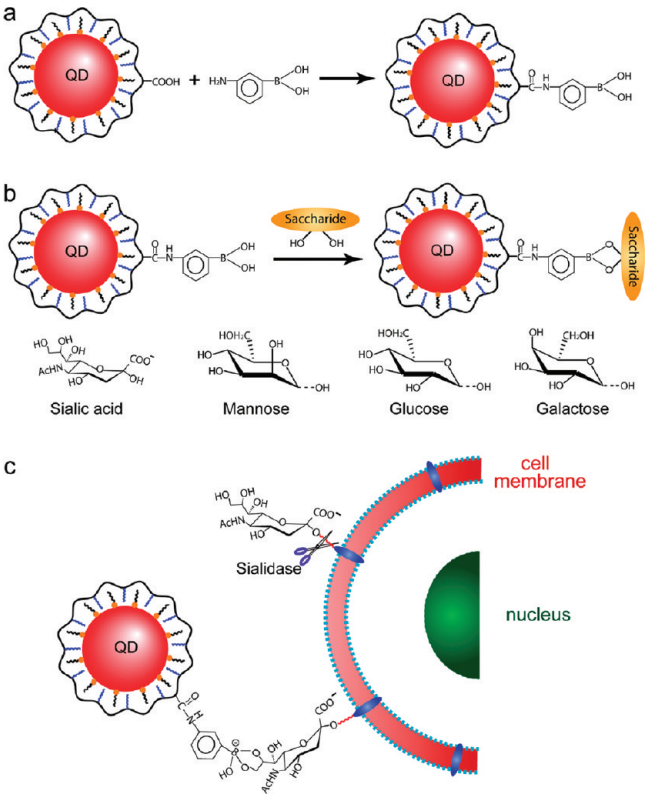

Figure 1. Schematic illustration of QD conjugation and the use of QD probes for specific labeling of SA on living cells. (a) Conjugation of carboxylic-acid functionalized QDs with 3-aminophenylboronic acid (APBA) by the EDAC-catalyzed reaction. (b) The reaction of phenylboronic acid (PBA) and diols in an aqueous solution. (c) Specific binding of QD with SA on living cells at the C-8, 9 diol of SA. The function of sialidase to remove SA moiety from glycans is illustrated as well.

achieved in exploiting bioconjugated QDs for labeling and tracking membrane proteins such as glycine receptor at neuronal surfaces[18,19] and various tumor associated receptors on cancer cells.[20,21] Therefore, the accessible SA molecules on cell surfaces are ideal imaging targets for QD probes.

Previous research by several groups has shown that PBA can reversibly react with 1,2 or 1,3 diols, which are abundant in glycan structures, to form five- or six-membered cyclic complexes.[22] Biosensors and glucose-triggered drug delivery systems have been developed on the basis of this reversible binding.[23] In general, the stable complex of PBA with diols in a favorable configuration can only form in its dissociated state at pH close to its pK_a (Figure 1a), which is typically about 8 to 9 for the commonly available PBA derivatives. However, a recent report by Kataoka et al. suggests that PBA forms favorable binding with SA among common carbohydrates (mannose, glucose, galactose, and SA) on cell surfaces at the physiological pH of 7.4.[22] This interesting finding provides an innovating molecular targeting platform for labeling SA on living cells. Very recently, the specific recognition of PBA-modified gold electrodes with SA has been used to detect SA on living cells in a potentionmetric method.[24] In current work, PBA targeting ligand was linked on QDs with carboxylic acid surface functionality by the carbodiimide-catalyzed reaction with 3-aminophenylboronic acid (APBA; Figure 1b). Our results have shown that the use of PBA-functionalized QDs enables one-step labeling and continuous tracking of the cell surface SA moieties of untreated living PC12 cells, which are neuroendocrine cells with abundant SA on their cell membranes mediating various cell functions such as cell adhesion, differentiation, and secretion.[25−28] The one-step procedure with fast kinetics and the biocompatibility of these QDs make it an ideal noninvasive technology for living cell imaging. The specificity of QD binding is confirmed by the competitive assay with free SA and staining of cells treated with sialidase, which removes the SA moiety from glycans (Figure 1c). We also find that the labeled SAs undergo quick internalization shortly after surface binding via endocytosis and eventually distribute in the perinuclear region. This distribution pattern is consistent with the notion that sialylated glycoproteins are populated on cell membranes and recycled through the vesicular exocytotic and endocytic pathways.[9,12] Furthermore, the single-particle imaging and quantitative analysis demonstrate the potential of the use of these QD probes to investigate diffusion dynamics of SA, which has been a significant challenge for glycan imaging.

EXPERIMENTAL SECTION

Preparation and Characterization of QD−PBA Conjugates. Core−shell QDs (CdSe/CdS/ZnS) were synthesized as previously described.[29] QDs coated with the amphiphilic copolymer of maleic anhydride and octadecene (PMO) were prepared following a standard protocol we developed previously.[30]

For QD−PBA conjugate preparation, 36 μM stock solution of QD−PMO was mixed with 1 mg/mL APBA dispersed in a 50 mM borate buffer solution (pH 7.4) and gently stirred for 2 to 3 min. After that, 10 mg/mL *N*-Ethyl-*N*′-(3-dimethylaminopropyl)-carbodiimide hydrochloride (EDAC) was added into the above mixture to start the EDAC-catalyzed coupling between PBA and QD−PMO. The reaction was carried out for about 4 h at room temperature. The molar ratios of QD−PBA−EDAC were controlled to be 1/4000/6000. The obtained samples were ultrafiltrated twice (5000 rpm for 5 min) to remove free unconjugated APBA. The concentration of APBA in the filtrate was measured by matching its absorption maximum at 291 nm to a predetermined standard curve, and the obtained results were used to calculate the number of APBA linked to QDs, leading to an average number of 850 PBA groups per QD (see Supporting Information). We found that two times of the ultrafiltration were sufficient to collect all the free APBA molecules, and the result was calculated on the basis of three parallel experiments. QD−PBA complexes conjugated with different monosaccharides (10 mM SA, mannose, glucose, and galactose) with a feeding molar ratio of QD−PBA to monosaccharides of 1:60 000 were prepared by the same procedure.

Spectroscopic properties of QD−PBA were characterized by UV−vis and fluorescence spectroscopy. QD concentrations were determined on the basis of a molar extinction coefficient of 2.5 × 10^5 $M^{-1}cm^{-1}$ at 610 nm. The excitation wavelength of fluorescence spectrum was 450 nm. Transmission electron microscope (TEM) observations were conducted on a Jeol JEM 2010 electron microscope at an acceleration voltage of 200 kV. The zeta potential of QDs was measured using a Malvern Nanozeta sizer (NanoZS 90).

Gel Electrophoresis. The loading capacity of QD−PBA for different monosaccharides was evaluated by gel electrophoresis (Thermo Scientific EC 300XL) in 1% agarose gels using 1× 3-(*N*-morpholino)propanesulfonic acid (MOPS; pH 7.4) as the running buffer at 100 V for 30 min.

Cell Culture, Imaging, and QD Cytotoxicity. PC 12 cells were incubated in RPMI 1640 medium (Invitrogen Corporation) with 10% fetal bovine serum, 5% horse serum, and 1% streptomycin for 2 to 3 days (37 °C, 5% CO_2). The living cells

dx.doi.org/10.1021/ac1028853 |*Anal. Chem.* 2011, 83, 1124–1130

without terminal SA residues in their glycans were obtained by culturing the cells (10^6 cells/mL) in a reduced serum RPMI 1640 medium including 40 mU/mL sialidase for about 30 min at 37 °C and followed by washing twice with 1× phosphate buffered solution (PBS, pH 7.4). The sialidase was usually utilized as a cleaving agent for all forms of SA components present on the carbohydrates of the cell surfaces. Treated and untreated PC 12 cells were seeded in 8-well LabTek chambers (Nalgene Nunc) with a concentration of 10^6 cells/mL for imaging experiments.

Fluorescence imaging of cells was carried out using a confocal microscope (Zeiss LSM 510 with a 63× oil objective) with the laser excitation wavelength of 488 nm at room temperature. The background fluorescence was modulated by incubating the living cells in a bathing solution (150 mM NaCl, 5 mM KCl, 1.1 mM $MgCl_2$, 2.6 mM $CaCl_2$, 10 mM HEPES, and 10 mM glucose, pH 7.4). Twenty nanomolar QD probes were used in our cell imaging. For the competitive assay, free SA (10 mM) was added to the living cells and incubated for about 10 min, followed by the addition of QD−PBA probes. SA-specific triticum vulgans lectin (0.01 mg/mL) labeled with fluorescein 5(6)-isothiocyanate (FITC) was also used to further validate SA distribution on the cell surfaces. Both fluorescence and bright-field images of labeled PC 12 cells were obtained for all samples. Single-cell spectroscopic detection was carried out in an Olympus71 inverted microscope with a PIXIS:100B spectroscopy CCD camera.

The motion of QD−PBA complexes on PC 12 cell plasma membrane was studied on an inverted total internal reflection fluorescence microscope (TIRFM) (Axiovert200, Carl Zeiss) equipped with a 100× oil-immersed object (1.45 NA) and an EMCCD camera. The 488 nm argon-ion laser was used for excitation, and a 620 nm emission filter used for detection. Time-lapse images of 241 frames (0.5 s/frame) were acquired at 37 °C and 2 Hz after 3 nM QD−PBA was incubated with the cells for 3 min and measured 20 min later. The trajectories of QDs were tracked using ImageJ (National Institute of Health) with the manual tracking plugin (http://rsbweb.nih.gov/ij/plugins/track/track.html) and analyzed by Igor (WaveMetrics). The velocity, diffusion coefficient, and mean square displacement (MSD) were calculated by analyzing 348 vesicles in 6 cells using a previously reported method.[31]

QDs cytotoxicity was evaluated using a standard cell counting Kit-8 (CCK-8) assay in a 96-well plate (5000 cells/well). After incubating 24 h in a humidified incubator (37 °C, 5% CO_2), QD−PMO and QD−PBA with final concentrations of 5 and 20 nM were added to the wells and incubated with the PC 12 cells for 4 h in the incubator. After that, CCK-8 solutions were added to each tested wells and incubated for 4 h. Since the absorbance of formazan (produced from the cleavage of CCK-8 by dehydrogenases in living cells) was directly proportional to the numbers of live cells, the absorbance of each sample at 450 nm was measured using a microplate reader and the morphology of all cells was observed using an optical microscope (Zeiss). The cell viability was calculated as the ratio of the absorbance of the sample well to that of the cell control and expressed as a percentage. All experiments were triplicated, and results were averaged.

RESULTS AND DISCUSSION

Core−shell QDs (CdSe/CdS/ZnS) with octadecylamine (ODA) capping ligands were synthesized using the method reported previously.[29] The hydrophobic QDs with 620 nm emission was encapsulated with amphiphilic copolymers of maleic anhydride and octadecene (PMO), leading to water-soluble QDs

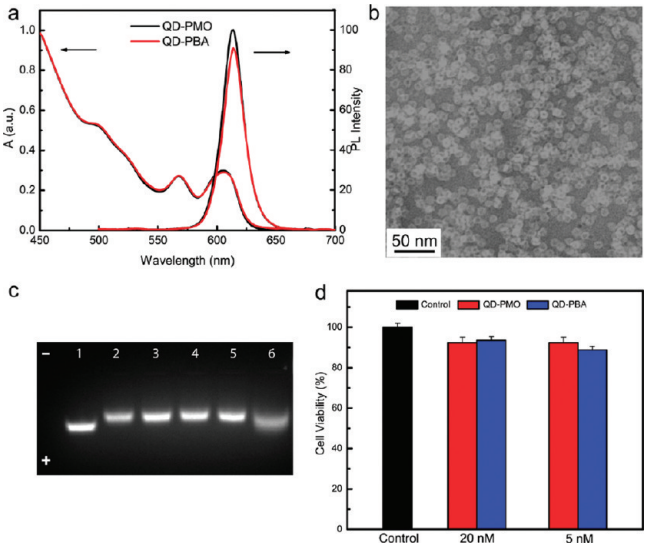

Figure 2. (a) Optical absorption and fluorescence emission spectra of QD−PMO and QD−PBA. (b) Transmission electron micrograph of negatively stained QD probes. (c) The binding of QD−PBA with different monosaccharides, including SA, glucose, mannose, and galactose, was tested by gel electrophoresis using the parent QD−PMO as a control: QD−PMO (lane 1), QD−PBA (lane 2), QD−PBA−mannose (lane 3), QD−PBA−glucose (lane 4), QD−PBA−galactose (lane 5), and QD−PBA−SA (lane 6). (d) Cell viability data of QD−PMO and QD−PBA obtained from cultured PC12 cells with the untreated cell as a control.

(QD−PMO) carrying carboxylic acid surface functionality.[30] To introduce PBA ligands, APBA was conjugated with the carboxylic acid groups in the presence of EDAC in pH 7.4 borate buffer. The straightforward EDAC-catalyzed coupling has been widely used for introducing protein or peptide ligands on QD surfaces. Because multiple functional groups (amines and carboxylic acids) are present within the proteins, careful optimization is necessary to minimize interparticle cross-linking and aggregation of the probes. The use of monofunctional small molecule (APBA) in this study avoids the occurrence of QD cross-linking, and the reaction has over 90% yields of QDs after removing unreacted APBA through ultrafiltration. As shown in Figure 2a, the spectroscopic properties (absorption profile, emission wavelength, and quantum yield) of these QDs (QD−PBA) have little change after the reaction, and the probes are highly stable in buffer solutions. Negatively stained images from transmission electron microscopy (TEM) reveals that the 6 nm QDs are surrounded by a uniform layer of polymer coating of 3 to 4 nm in thickness (Figure 2b).

The PMO coated QDs are negatively charged with a zeta potential of −32 mV due to the presence of a large amount of carboxylic groups. Partial conversion of carboxylic acid to PBA leads to reduced zeta potential (−19 mV) at pH 7.4 due to the higher pK_a (8 to 9) of PBA than that (5 to 6) of the carboxylic acid group in PMO copolymers. The average number of PBA ligands on each QD is about 850. The introduction of small molecules such as APBA is expected to have little impact on the QD sizes. Therefore, the lower electrophoretic mobility (Figure 2c) of QD−PBA than the parent QD−PMO should result from the decrease in surface charges. The binding of QD−PBA with the primary monosaccharides on cell surfaces was also examined with gel electrophoresis, which has shown that addition of SA increases the gel mobility of QDs, while the QDs incubated with glucose, mannose, and galactose exhibit almost identical migration as

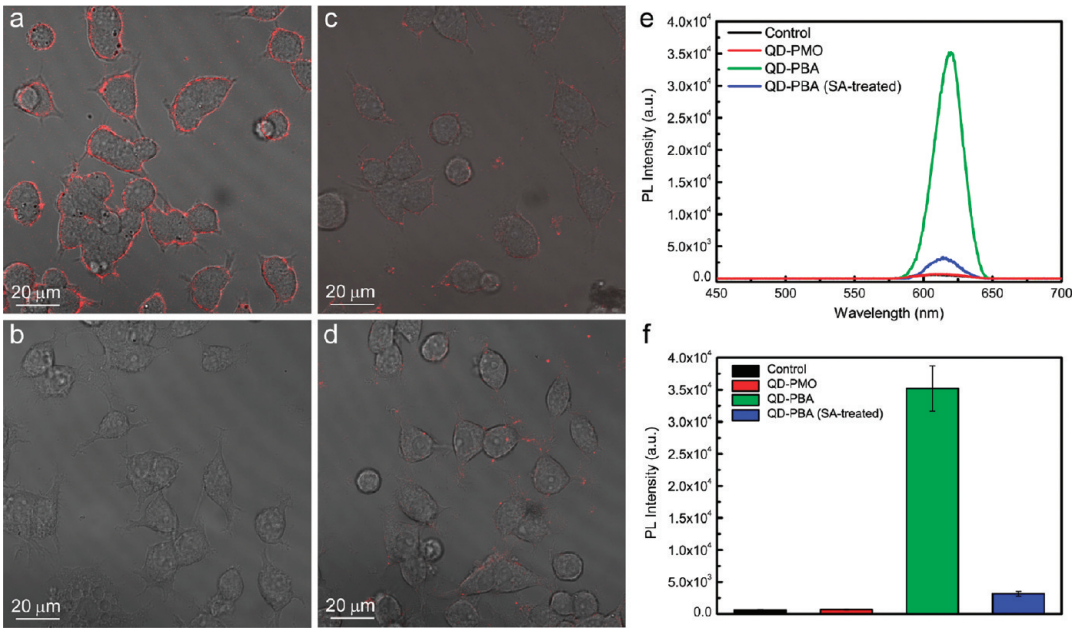

Figure 3. Overlaid fluorescence and bright field confocal microscopy images of living PC 12 cells incubated with three types of QD probes. (a) QD−PBA, (b) QD−PMO, (c) QD−PBA with 10 mM free SA, and (d) QD−PBA. (Cells were treated with sialidase to remove SA on the cell membrane.) Single cell fluorescence spectra (e) and average fluorescence intensity (f) of single cells in the corresponding cell samples.

QD−PBA. As discussed above, the PBA−saccharide complexes are preferentially formed at the dissociated state of PBA, which is negatively charged. The gel migration data indicate that QD−PBA has selectivity toward SA over other types of monosaccharides. This is also consistent with the previous report by Kataoka and co-workers, which shows that the PBA−SA complex has higher binding affinity than those of glucose, mannose, and galactose at pH 7.4.[22] For example, the equilibrium constant of PBA binding to SA is over 7 times of that to glucose. In the complex of QD−PBA and SA, the associated C-1 carboxylic acid group of SA would contribute to the increase of surface charge and corresponding electrophoretic mobility, as shown in Figure 2c.[22,32]

One of the major concerns of the use of QDs for living cell and in vivo applications are their potential toxicity associated with cadmium ions. Bhatia et al. reported that cadmium-based QDs are highly toxic to cells due to the release of cadmium ions under extensive UV illumination.[33] However, accumulating evidence has shown that rationally designed surface coatings can protect QDs from degradation. Several groups including us have used QDs with PMO coating for various living cell and in vivo imaging experiments, and these QDs are stable enough to survive regular imaging experiments.[17,21] Cytotoxicity may also arise from their surface functionalities. For example, QDs with cationic surface charges display significantly higher cytotoxic effect than those with anionic surface charge due to their electrostatic interactions with negatively charged glycocalyx on cell membranes.[34] Our results (Figure 2d) with QD−PBA suggest that introducing PBA functionality did not change the cytotoxicity profile of QDs on PC12 cells. The cells maintained over 90% viability after incubation with these QD probes at the two concentrations we used for imaging experiments, and the cell morphology also did not show any visible alteration compared to the control cells.

In living cell imaging, QD−PBA was evaluated for binding with SA on PC12 cells, which is known to express SA on the cell membrane.[25,26] The cell membrane is visibly stained within 1 min of QD−PBA addition, as shown in confocal microscopy images (Figure 3a), whereas the precursor QD−PMO probes do not lead to any detectable labeling (Figure 3b) after much longer incubation. To further verify the staining observed is indeed due to the specific recognition between PBA ligands and cell surface SA receptors, free SA (10 mM) was added for binding competition. It is clear that the addition of free SA can effectively inhibit the QD binding on cell surfaces (Figure 3c), indicating QD−PBA probes do have strong binding with SA. More importantly, removal of cell surface SA moieties with 30 min sialidase treatment led to dramatic reduction in cell staining, providing conclusive evidence to support the excellent targeting ability of the small molecular ligand. Furthermore, a similar SA distribution pattern (see Supporting Information) was also revealed with SA-specific triticum vulgans lectin labeled with FITC.[35] Single-cell fluorescence spectrometry (Figure 3e,f) provides quantitative comparison for the degree of labeling. The average fluorescence intensity of QD−PMO treated and the control cells are about 2% of that of the QD−PBA labeled ones, and the sialidase-treatment leads to more than 90% drop of labeling, further confirming the selectivity observed in fluorescence imaging.

One major advantage of the one-step QD labeling with fast binding kinetics is the elimination of the complicated pretreatment of living cells in the previously reported methods and the associated cytotoxic effects.[9−13] It is likely that the presence of 850 PBA ligands in the nanosized probes gives rise to the multivalent interaction between PBA and SA, which could further improve the binding affinity and specificity.[36] We notice that QDs with PBA groups have recently been used for fluorescence resonance energy transfer-based nanosensors for detection of molecules with diols including saccharides.[37,38] To develop targeting ligands for carbohydrates other than SA on cell surfaces and similar nanosensors for living cell applications, it would be necessary to design new PBA derivatives with specific binding to the carbohydrate target of interests at physiological pH.

To investigate how QD probes enter the endocytic pathways together with SA, a serial of time-dependent (up to 90 min)

dx.doi.org/10.1021/ac1028853 |*Anal. Chem.* 2011, 83, 1124–1130

confocal images of PC12 cells incubated with QD−PBA probes were recorded (Figure 4). In the first 10 min of incubation, an increasing amount of QDs was bound to the cell membrane, forming a uniform ring-shaped fluorescence pattern. At 20 min, QDs start to appear inside the cells, but the majority of the QDs still remain on the cell membrane. In contrast to the initial homogeneous staining, clusters of QDs are observed on the cell membrane. From 20 to 60 min, more and more QDs were internalized and found in the intracellular space. The intracellular punctuate distribution pattern of QDs and the considerably brighter fluorescence of the individual dots than single QDs suggest that nearly all of the QDs were segregated into vesicles instead of individually dispersed in the cytosol.[39,40] A longer incubation time did not change the distribution pattern of QDs. Our findings are in line with previous reports on localization of the glycosylation machinery, which demonstrates that sialylated moieties are organized on the cell membrane and reside in the intracellular organelles along the exocytotic and endocytic pathways.[9] QD probes are considerably larger than small molecular fluorophores used previously in glycan labeling. These results suggest that QD labels did not significantly perturb glycan trafficking on the time scale of the experiment.

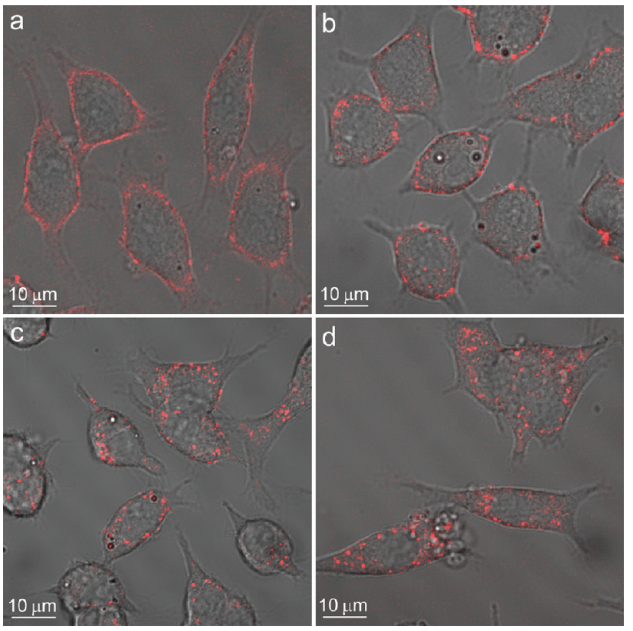

Figure 4. Overlaid fluorescence and bright field images of time-dependent living cell labeling of QD−PBA and the intracellular distribution of QD−labeled sialic acids. (a) 10 min, (b) 20 min, (c) 60 min, and (d) 90 min.

Clusters of QDs observed at 20 min on the cell membrane indicate that SA on the membrane experience reorganization prior to internalization. To track the motion of QD−labeled SA on cell membrane in this process, we recorded sequences of time-lapse fluorescence images (0.5 s/frame) using total internal reflection fluorescence microscopy (TIRFM; Figure 5), which has emerged as a powerful imaging technique to study molecular events in the thin subplasmalemmal region (<200 nm in thickness).[31,41,42] The majority of the tracked trajectories of QD labeled SA do not show the on−off fluorescence blinking that single QD features (see Supporting Information Movie S1),

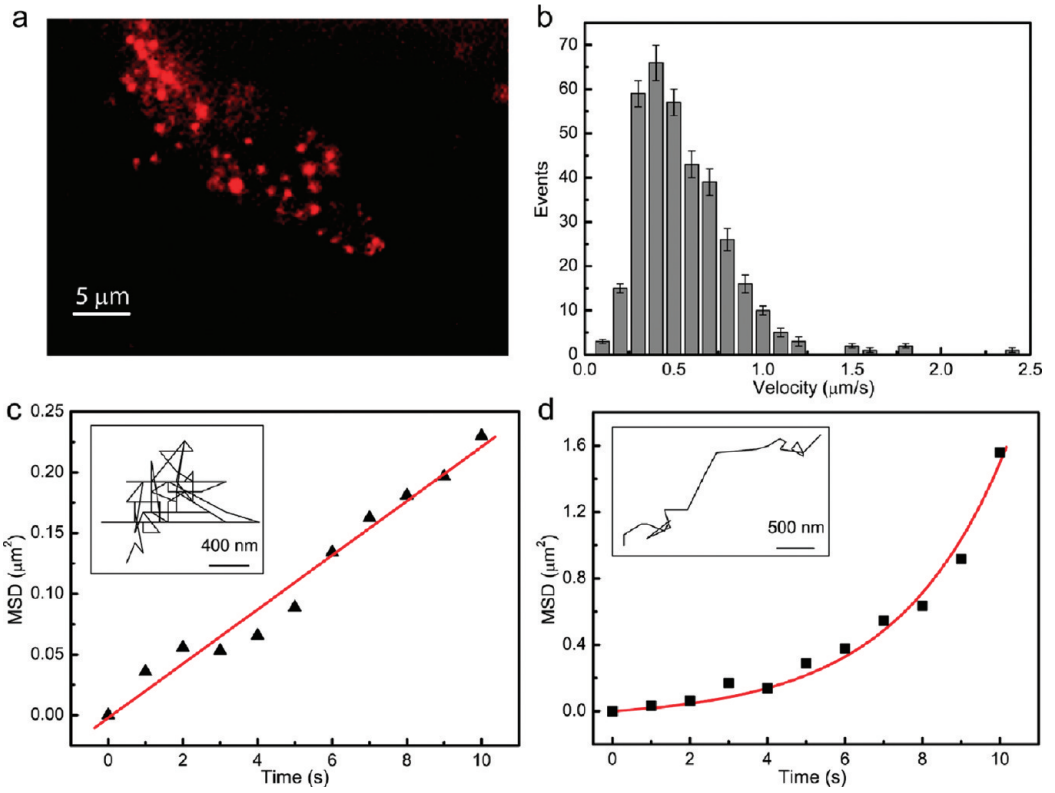

Figure 5. (a) TIRFM imaging of QD labeled SA in the thin subplasmalemmal region of living cells. (b) Diffusion velocity distribution of QDs obtained by tracking 348 trajectories in 6 cells with the duration of 2 min (0.5 s/frame). Time dependence of MSD reveal Brownian (c) and directed motion (d) regimes (Insets: typical lateral movement trajectories).

dx.doi.org/10.1021/ac1028853 |*Anal. Chem.* 2011, 83, 1124–1130

confirming that QDs form clusters as shown in the confocal images (Figure 4b). This is in agreement with the view that endocytosis occurs at defined functional membrane domains.[43,44] Tracking of 348 trajectories in 6 cells gives rise to a mean diffusion velocity of 0.56 ± 0.04 μm/s (Figure 5b). The analysis on MSD curves (Figure 5c,d) reveals two major types of diffusion regimes, in which 88% of them are in Brownian motion, indicated by the linear MSD plot, and the rest are in directed motion, evidenced by linear trajectories and the corresponding quadratic MSD curves.[45] Taken together, it is clear that the use of brightly stable QD probes with PBA targeting ligands allows for revealing abundant information about sialylated glycans in live cell including localization, expression level, trafficking, and diffusion dynamics on cell membranes, although further experiments are necessary to achieve a comprehensive understanding on the interplay of sialylated proteins/lipids and other membrane components during the endocytosis and exocytosis.[46,47]

CONCLUSIONS

In summary, we have reported a new class of QD probes for labeling and tracking of SA on living cell with the high specificity built upon a novel small molecular borate ligand for SA. The use of biocompatible QD-based probes allows for long-term tracking of the sialylated glycoproteins and reveals their intracellular distribution, trafficking, and diffusion dynamics on cell membrane. This work also suggests the potential of borate derivatives to target other primary carbohydrates on cell surfaces. The combination of multicolor QDs and individual borate ligands targeting specific carbohydrates would open a new avenue to uncover the complex glycosylation machinery and related membrane organization and cell functions.

ASSOCIATED CONTENT

Supporting Information. Additional information as noted in text. This material is available free of charge via the Internet at http://pubs.acs.org.

AUTHOR INFORMATION

Corresponding Author
*E-mail: hduan@ntu.edu.sg.

ACKNOWLEDGMENT

H.D. acknowledges the program of Nanyang Assistant Professorship for financial support. This work is supported in part by Tier 2 grant (T206B3220) to P.C. from the Ministry of Education (Singapore). We are grateful to Y. A. Wang at OceanNanotech for helpful discussion.

REFERENCES

(1) Raman, R.; Raguram, S.; Venkataraman, G.; Paulson, J. C.; Sasisekharan, R. *Nat. Methods* **2005,** *2*, 817–824.
(2) Chen, X.; Varki, A. *ACS Chem. Biol.* **2010,** *5*, 163–176.
(3) Schauer, R. *Glycoconjugate J.* **2000,** *17*, 485–499.
(4) Varki, A. *Trends Mol. Med.* **2008,** *14*, 351–360.
(5) Lindberg, G.; Eklund, G. A.; Gullberg, B.; Rastam, L. *Br. Med. J.* **1991,** *302*, 143–146.
(6) Marquina, G.; Waki, H.; Fernandez, L. E.; Kon, K.; Carr, A.; Valiente, O.; Perez, R.; Ando, S. *Cancer Res.* **1996,** *56*, 5165–5171.
(7) Alfonso, M.; Diaz, A.; Hernandez, A. M.; Perez, A.; Rodriguez, E.; Bitton, R.; Perez, R.; Vazquez, A. M. *J. Immunol.* **2002,** *168*, 2523–2529.
(8) Wang, S. S. S.; Rymer, D. L.; Good, T. A. *J. Biol. Chem.* **2001,** *276*, 42027–42034.
(9) Zeng, Y.; Ramya, T. N. C.; Dirksen, A.; Dawson, P. E.; Paulson, J. C. *Nat. Methods* **2009,** *6*, 207–209.
(10) Laughlin, S. T.; Baskin, J. M.; Amacher, S. L.; Bertozzi, C. R. *Science* **2008,** *320*, 664–667.
(11) Hangauer, M. J.; Bertozzi, C. R. *Angew. Chem., Int. Ed.* **2008,** *47*, 2394–2397.
(12) Baskin, J. M.; Prescher, J. A.; Laughlin, S. T.; Agard, N. J.; Chang, P. V.; Miller, I. A.; Lo, A.; Codelli, J. A.; Bertozzi, C. R. *Proc. Natl. Acad. Sci. U.S.A.* **2007,** *104*, 16793–16797.
(13) Czlapinski, J. L.; Bertozzi, C. R. *Curr. Opin. Chem. Biol.* **2006,** *10*, 645–651.
(14) Alivisatos, A. P.; Gu, W. W.; Larabell, C. *Annu. Rev. Biomed. Eng.* **2005,** *7*, 55–76.
(15) Smith, A. M.; Nie, S. M. *Acc. Chem. Res.* **2010,** *43*, 190–200.
(16) Michalet, X.; Pinaud, F. F.; Bentolila, L. A.; Tsay, J. M.; Doose, S.; Li, J. J.; Sundaresan, G.; Wu, A. M.; Gambhie, S. S.; Weiss, S. *Science* **2005,** *307*, 538–544.
(17) Smith, A. M.; Duan, H. W.; Mohs, A. M.; Nie, S. M. *Adv. Drug Delivery Rev.* **2008,** *60*, 1226–1240.
(18) Dahan, M.; Levi, S.; Luccardini, C.; Rostaing, P.; Riveau, B.; Triller, A. *Science* **2003,** *302*, 442–445.
(19) Gussin, H. A.; Tomlinson, I. D.; Little, D. M.; Warnement, M. R.; Qian, H. H.; Rosenthal, S. J.; Pepperberg, D. R. *J. Am. Chem. Soc.* **2006,** *128*, 15701–15713.
(20) Gao, X. H.; Cui, Y. Y.; Levenson, R. M.; Chung, L. W. K.; Nie, S. M. *Nat. Biotechnol.* **2004,** *22*, 969–976.
(21) Yang, L. L.; Mao, H.; Wang, Y. A.; Cao, Z. H.; Peng, X. H.; Wang, X. X.; Duan, H. W.; Ni, C. C.; Yuan, Q. G.; Adams, G.; Smith, M. Q.; Wood, W. C.; Gao, X. H.; Nie, S. M. *Small* **2009,** *5*, 235–243.
(22) Otsuka, H.; Uchimura, E.; Koshino, H.; Okano, T.; Kataoka, K. *J. Am. Chem. Soc.* **2003,** *125*, 3493–3502.
(23) Nakayama, D.; Takeoka, Y.; Watanabe, M.; Kataoka, K. *Angew. Chem., Int. Ed.* **2003,** *42*, 4197–4200.
(24) Matsumoto, A.; Sato, N.; Kataoka, K.; Miyahara, Y. *J. Am. Chem. Soc.* **2009,** *131*, 12022–12023.
(25) Kontou, M.; Bauer, C.; Reutter, W.; Horstkorte, R. *Glycoconjugate J.* **2008,** *25*, 237–244.
(26) Vale, R. D.; Hosang, M.; Shooter, E. M. *Dev. Neurosci.* **1985,** *7*, 55–64.
(27) Sudibya, H. G.; Ma, J. M.; Dong, X. C.; Ng, S.; Li, L. J.; Liu, X. W.; Chen, P. *Angew. Chem., Int. Ed.* **2009,** *48*, 2723–2726.
(28) Ma, J. M.; Zhao, Y. Y.; Ng, S.; Zhang, J.; Zeng, J.; Than, A.; Chen, P.; Liu, X. W. *Chem.—Eur. J.* **2010,** *16*, 4533–4540.
(29) Duan, H. W.; Kuang, M.; Wang, Y. A. *Chem. Mater.* **2010,** *22*, 4372–4378.
(30) Duan, H. W.; Kuang, M.; Wang, X. X.; Wang, Y. A.; Mao, H.; Nie, S. M. *J. Phys. Chem. C* **2008,** *112*, 8127–8131.
(31) Pinaud, F.; Michalet, X.; Iyer, G.; Margeat, E.; Moore, H. P.; Weiss, S. *Traffic* **2009,** *10*, 691–712.
(32) Djanashvili, K.; Frullano, L.; Peters, J. A. *Chem.—Eur. J.* **2005,** *11*, 4010–4018.
(33) Derfus, A. M.; Chan, W. C. W.; Bhatia, S. N. *Nano Lett.* **2004,** *4*, 11–18.
(34) Duan, H. W.; Nie, S. M. *J. Am. Chem. Soc.* **2007,** *129*, 3333–3338.
(35) Charland, N.; Kellens, J. T. C.; Caya, F.; Gottschalk, M. *J. Clin. Microbiol.* **1995,** *33*, 2220–2221.
(36) Hong, S.; Leroueil, P. R.; Majoros, I. J.; Orr, B. G.; Baker, J. R.; Holl, M. M. B. *Chem. Biol.* **2007,** *14*, 107–115.
(37) Freeman, R.; Willner, I. *Nano Lett.* **2009,** *9*, 322–326.
(38) Freeman, R.; Bahshi, L.; Finder, T.; Gill, R.; Willner, I. *Chem. Commun.* **2009,** 764–766.
(39) Ruan, G.; Agrawal, A.; Marcus, A. I.; Nie, S. M. *J. Am. Chem. Soc.* **2007,** *129*, 14759–14766.
(40) Delehanty, J. B.; Medintz, I. L.; Pons, T.; Brunel, F. M.; Dawson, P. E.; Mattoussi, H. *Bioconj. Chem.* **2006,** *17*, 920–927.

(41) Zhang, J.; Xue, R. H.; Ong, W. Y.; Chen, P. *Biophys. J.* **2009,** *97,* 1371–1380.
(42) Soo, J. C.; Zhang, J.; He, Q. Y.; Agarwal, S.; Li, H.; Zhang, H.; Chen, P. *Integr. Biol. UK* **2010,** *2,* 250–257.
(43) Parton, R. G.; Richards, A. A. *Traffic* **2003,** *4,* 724–738.
(44) Nichols, B. *J. Cell Sci.* **2003,** *116,* 4707–4714.
(45) Courty, S.; Luccardini, C.; Bellaiche, Y.; Cappello, G.; Dahan, M. *Nano Lett.* **2006,** *6,* 1491–1495.
(46) Delehanty, J. B.; Mattoussi, H.; Medintz, I. L. *Anal. Bioanal. Chem.* **2009,** *393,* 1091–1105.
(47) Kusumi, A.; Nakada, C.; Ritchie, K.; Murase, K.; Suzuki, K.; Murakoshi, H.; Kasai, R. S.; Kondo, J.; Fujiwara, T. *Annu. Rev. Biophys. Biomol. Struct.* **2005,** *34,* 351–378.